O(N) LDA+U electronic structure calculation method based on the nonorthogonal pseudoatomic orbital basis

Myung Joon Han,[1] Taisuke Ozaki,[2] and Jaejun Yu[1,3,*]
[1]*School of Physics and CSCMR, Seoul National University, Seoul 151-747, Korea*
[2]*RICS-AIST, 1-1-1 Umezono, Tsukuba, Ibaraki 305-8568, Japan*
[3]*Center for Theoretical Physics, Seoul National University, Seoul 151-747, Korea*
(Received 26 August 2005; revised manuscript received 26 October 2005; published 13 January 2006)

We report an implementation of the LDA+U method based on the state-of-the-art linear combination of pseudo-atomic orbital (LCPAO) method, which is suitable for large-scale O(N) electronic structure calculations based on the density functional theory. By introducing a *dual* representation of the occupation number matrix instead of the *on-site* or *full* representations, the LDA+U formalism is refined to be consistent with a nonorthogonal LCPAO basis in regard to the sum rule of the total number of electrons. For typical transition metal oxide bulk systems, the band gap, magnetic moment, and detailed electronic structures are investigated with the different choices of basis orbitals and effective U values as well as the definition of the occupation number matrix. The results are in good agreement with previous theoretical and experimental studies, indicating that the proposed LDA+U scheme combined with the O(N) method is a quite promising approach for the study of large-scale correlated material systems consisting of localized electrons. We discuss the electronic structure and magnetic properties of $(NiO)_m/(CoO)_n$ superlattices as an application of our method.

DOI: 10.1103/PhysRevB.73.045110 PACS number(s): 71.15.−m, 71.15.Ap, 71.15.Mb, 71.20.Be

I. INTRODUCTION

Since its first suggestion by Hohenberg, Kohn, and Sham,[1,2] the density functional theory (DFT) combined with local density approximation (LDA) or generalized gradient approximation (GGA) have made a great success in the description of ground state and related properties without any adjustable parameter.[3,4] However, due to the simplification in their exchange-correlation (XC) functional form and other unphysical features like self-interactions, LDA and GGA fail to describe the system with strong Coulomb interactions such as transition metal oxides and rare-earth compounds.[5–9] Several attempts have been devoted to improving this primitive LDA approximation and its GGA extension in order to extend the applicability of the DFT to the systems with strong electron correlations. One of the developments toward improving LDA is to merge LDA with a model-based many-body technique such as Hubbard model[10] and dynamical mean-field theory (DMFT).[11] GW and self-interaction correction (SIC) are other examples[5] by including the many-body self-energy terms (GW) or excluding the unphysical self-interactions (SIC).[5]

Among various approaches, the LDA+U method[5,12] has made a success in understanding strongly correlated systems partly due to its simplistic treatment of the on-site Coulomb correlation effect and the modest computational time as a result. In principle the LDA+U approach requires only the same scale of computational cost with LDA because of the local correction in real space. From the point of view regarding the description of large-scale correlated systems, LDA+U can be considered as one of the most efficient approaches.

Meanwhile the development of methodology reducing the computational cost is another important issue in first-principles DFT calculations. For example, there have been great efforts to develop a linear-scaling method, so called O(N) method,[13–19] and to make efficient basis orbitals.[20–27] The use of linear-combination-of-pseudo-atomic-orbital (LCPAO) methods, i.e., localized basis functions with a vanishing tail, enables us not only to reduce the computational cost but also to be more adequate for using various O(N) algorithms. Along with recent advances of bioscience and nanotechnology, the applicability of DFT to realistic large-scale systems at nanometer scale and in biological molecules becomes more demanding.

While there have been several implementations of LDA+U into the linear muffin-tin orbital (LMTO) method,[12] full-potential linearized augmented plane-wave (FLAPW) method,[28] projector augmented-wave (PAW) method,[29] pseudopotential-plane-wave method,[30] and full-potential local-orbital method,[31] not much progress has been made in the LDA+U LCPAO method[20,21,26] toward O(N) calculations. The LDA+U method combined with the LCPAO basis may have significance in extending the applicability of DFT to the large-scale system with strong Coulomb correlations. In addition, the extraction of tight-binding parameters is natural within the LCPAO formalism and its application to DMFT calculations is highly plausible too.

In this paper we report our implementation of LDA+U into the state-of-the-art LCPAO method and present our refinement of LDA+U formalism for the nonorthogonal atomic orbital basis. Results of our calculations applied to typical transition metal oxide (TMO) bulk systems are in good agreement with experimentals as well as the previous calculations in the band structure, band gap, and magnetic moment. It is noted that, although the use of a local orbital is natural for the implementation of LDA+U methods, there has been some ambiguity in the definition of occupation number within the nonorthogonal linear-combination-of-atomic-orbitals (LCAO) basis.[32] We attempt to resolve this

issue by introducing a *dual* representation of the occupation number matrix. The suggested *dual* representation not only preserves the original concept of atomic density but also satisfies the sum rule. We compare the physical quantities obtained by introducing the *dual* representation with those by using other definitions suggested before. We also investigate how the choice of the LCPAO basis such as multiple zeta and polarization orbitals affect the electronic structure obtained by the LDA+U calculations.

II. FORMALISM

A. LDA+U total energy functional

The problem of LDA in the description of localized d- and f-electrons in transition metal oxides and rare-earth compounds, which is related to the band gap, local moment, and orbital polarization, is mainly attributed to the LDA treatment of the Coulomb interactions among electrons. A prescription to cure such a failure is to introduce an orbital-dependent functional. The LDA+U method[6] is one of the simple orbital-dependent functionals in which a generalized Hubbard model is introduced in order to treat the localized d and f electrons based on the unrestricted Hartree-Fock theory. Then, in conjunction with the generalized Hubbard model, the LDA+U total energy functional is given by adding the energy E_U^0 of a generalized Hubbard model for the localized electrons to the LDA functional and by subtracting a double counting energy E_{dc}^U of the localized electrons described in a mean-field sense:[5,6]

$$E_{\mathrm{LDA}+U} = E_{\mathrm{LDA}} + E_U^0 - E_{\mathrm{dc}}^U, \tag{1}$$

where E_U^0 is given by a spherically averaged screened-Coulomb energy U and exchange energy J:

$$E_U^0 = \frac{1}{2}\sum_\alpha U_\alpha \sum_{\sigma m m'} n_{\alpha m}^\sigma n_{\alpha m'}^{-\sigma} + \frac{1}{2}\sum_\alpha (U_\alpha - J_\alpha) \sum_{\sigma, m\neq m'} n_{\alpha m}^\sigma n_{\alpha m'}^\sigma, \tag{2}$$

where σ is the spin index, and $\alpha \equiv (ilp)$ with the site index i, angular momentum quantum number l, and multiplicity number of radial basis function p. $n_{\alpha m}^\sigma$ is an eigenvalue of the occupation number matrix to be discussed later on. Here U and J values are assumed to be dependent only on the index α, but independent of the azimuthal quantum number m, which is regarded as a simplification to the Hartree-Fock theory by a spherical average.[33] In this study the U- and J-values are treated as adjustable parameters rather than quantities derived from the first-principles calculation such as a constrained DFT approach.

One possible choice of the double counting term E_{dc}^U is[33]

$$E_{\mathrm{dc}}^U = \frac{1}{2}\sum_\alpha U_\alpha N_\alpha (N_\alpha - 1) - \frac{1}{2}\sum_\alpha J_\alpha \sum_\sigma N_\alpha^\sigma (N_\alpha^\sigma - 1), \tag{3}$$

where $N_\alpha^\sigma = \Sigma_m n_{\alpha m}^\sigma$ and $N_\alpha = N_\alpha^\uparrow + N_\alpha^\downarrow$. It is noted that the expression in Eq. (3) for the double counting term is also derived by assuming an integer occupation number, 0 or 1, in the atomic limit. Thus the form is expected to be suitable for highly localized d and f electrons. Another possible way is to estimate the double counting term by assuming the uniform occupancy.[7] Although there is an attempt to bridging two limits:[8] the atomic limit with an integer occupation number and the mean field with the uniform occupancy, we adopt the atomic limit Eq. (3) as a double counting term because our main interest lies on TMO systems with highly localized d electrons. The energy correction $E_U \equiv E_U^0 - E_{\mathrm{dc}}^U$ to the LDA energy can be written by a penalty functional as follows:

$$E_U = \frac{1}{2}\sum_\alpha (U_\alpha - J_\alpha) \sum_\sigma \{\mathrm{Tr}(n_\alpha^\sigma) - \mathrm{Tr}(n_\alpha^\sigma n_\alpha^\sigma)\}. \tag{4}$$

If $(U_\alpha - J_\alpha)$ is positive, the energy correction always imposes a positive penalty on the total energy except for the case with a diagonal integer occupation number 0 or 1, which means that the state with an integer occupation number is stabilized, leading to the orbital polarization. It is easy to verify that the derivative of the functional with respect to N_α^σ is discontinuous at an integer N_α^σ, since the diagonal occupation number $n_{\alpha m}^\sigma$ varies from 0 to 1 in principle. Unlike the LDA and GGA this feature is consistent with the condition that the exact exchange-correlation functional should possess.[9] It is convenient to define an effective Coulomb energy as $\bar{U}_\alpha \equiv (U_\alpha - J_\alpha)$, since only the difference $(U_\alpha - J_\alpha)$ is important in this spherically averaged but still rotationally invariant form of LDA+U energy correction.[12,33] Considering the use of multiple d and f orbitals and the rotational invariance of the energy correction, we can make a unitary transformation of Eq. (4) with respect to each subshell α:

$$\begin{aligned} E_U &= \frac{1}{2}\sum_\alpha \bar{U}_\alpha \sum_\sigma [\mathrm{Tr}(\mathsf{A}_\alpha n_\alpha^\sigma \mathsf{A}_\alpha^\dagger) - \mathrm{Tr}(\mathsf{A}_\alpha n_\alpha^\sigma \mathsf{A}_\alpha^\dagger \mathsf{A}_\alpha n_\alpha^\sigma \mathsf{A}_\alpha^\dagger)] \\ &= \frac{1}{2}\sum_\alpha \bar{U}_\alpha \sum_\sigma \left[\sum_m \mathsf{n}_{\alpha m m}^\sigma - \sum_{m m'} \mathsf{n}_{\alpha m m'}^\sigma \mathsf{n}_{\alpha m' m}^\sigma\right]. \end{aligned} \tag{5}$$

In Eq. (5), the off-diagonal terms within the subshell α of the occupation number matrix are taken into account, while those between subshells are neglected. This treatment is consistent with the functional used by Dudarev *et al.*,[33] and is a simple extension of the rotationally invariant functional for the case with different $\bar{U}$ values for different basis orbital index $\alpha \equiv (ilp)$. In this simple extension, we cannot only include multiple orbitals for the same angular momentum number l as the basis set, but also can easily derive the force on atoms in a simple form to be discussed later.

B. On-site density matrix in a dual representation

In Eq. (5), both the occupation numbers as well as the effective Coulomb energy $\bar{U}$ are crucial in determination of the correlation effects from a computational point of view. Although the localized basis orbitals in the LCPAO method can be readily adopted for the representation of the on-site interactions of the LDA+U formalism, however, there is some ambiguity in the definition of the occupation number matrix due to the nature of the nonorthogonality of localized basis orbitals. In this section three different definitions of the

occupation number matrix are compared and discussed in the perspective of the sum rule to be satisfied in a physical sense. In general, the on-site occupation number matrix $\mathsf{n}^{\sigma}_{\alpha}$ for the orbital α at the site i can be calculated from the density matrix $\hat{\rho}$ of the system by

$$\mathsf{n}^{\sigma}_{\alpha mm'} = \langle \alpha m\sigma|\hat{\rho}|\alpha m'\sigma\rangle. \tag{6}$$

Alternatively, the matrix element $\mathsf{n}^{\sigma}_{\alpha mm'}$ can be rewritten by introducing a local projection operator $\hat{P}^{\sigma}_{\alpha mm'} = |\alpha m'\sigma\rangle\langle\alpha m\sigma|$ for the (m,m')-th element of the occupation number matrix $\mathsf{n}^{\sigma}_{\alpha}$,

$$\mathsf{n}^{\sigma}_{\alpha mm'} = \mathrm{Tr}(\hat{\rho}\hat{P}^{\sigma}_{\alpha mm'}). \tag{7}$$

Then, within the Kohn-Sham (KS) formalism, we can evaluate the occupation number matrix $\mathsf{n}^{\sigma}_{\alpha mm'}$ by

$$\mathsf{n}^{\sigma}_{\alpha mm'} = \sum_{\mathbf{k}\nu} f(\epsilon^{\sigma}_{\mathbf{k}\nu})\langle\Psi^{\sigma}_{\mathbf{k}\nu}|\hat{P}^{\sigma}_{\alpha mm'}|\Psi^{\sigma}_{\mathbf{k}\nu}\rangle, \tag{8}$$

where $f(\epsilon)$ represents the Fermi-Dirac distribution function; $\Psi^{\sigma}_{\mathbf{k}\nu}$ and $\epsilon^{\sigma}_{\mathbf{k}\nu}$ are the KS eigenvector and eigenvalue for the momentum $\mathbf{k}$, band index ν, and spin index σ, respectively, and the summation over $\mathbf{k}$ implies the $\mathbf{k}$-space integration over the first Brillouin zone.

For the case of nonorthogonal basis orbitals, however, different sets of the occupation number matrices are expected to emerge from different choices of the local projection operators. First, we can think of two obvious choices of the local projectors:

$$\hat{P}^{\sigma}_{\alpha mm'}(\text{on-site}) = |\widetilde{\alpha m'\sigma}\rangle\langle\widetilde{\alpha m\sigma}|, \tag{9}$$

$$\hat{P}^{\sigma}_{\alpha mm'}(\text{full}) = |\alpha m'\sigma\rangle\langle\alpha m\sigma|, \tag{10}$$

which are called as *on-site* and *full* local projectors, respectively. For the on-site projection, a dual orbital $|\widetilde{\alpha m\sigma}\rangle$ of the original nonorthogonal basis orbital $|\alpha m\sigma\rangle$ is defined as

$$|\widetilde{\alpha m\sigma}\rangle = \sum_{\alpha' m'} S^{-1}_{\alpha m,\alpha' m'}|\alpha' m'\sigma\rangle, \tag{11}$$

so that the overlap matrix between nonorthogonal basis orbitals and the dual orbitals satisfy the following biorthogonal relation:

$$\langle\widetilde{\alpha m\sigma}|\alpha' m'\sigma'\rangle = \delta_{\alpha m\sigma,\alpha' m'\sigma'}. \tag{12}$$

For the use of the *on-site* and *full* local projectors, the corresponding occupation number matrices are given by

(i) *on-site*

$$\mathsf{n}^{\sigma}_{\alpha mm'} = \rho^{\sigma}_{\alpha m,\alpha m'}, \tag{13}$$

(ii) *full*

$$\mathsf{n}^{\sigma}_{\alpha mm'} = \sum_{\beta n,\beta' n'} \rho^{\sigma}_{\beta n,\beta n'} S_{\beta n,\alpha m} S_{\alpha m',\beta' n'}. \tag{14}$$

The density matrix element $\rho^{\sigma}_{\beta n,\beta' n'}$ can be evaluated by

$$\rho^{\sigma}_{\beta n,\beta' n'} = \langle\widetilde{\beta n\sigma}|\hat{\rho}|\widetilde{\beta' n'\sigma}\rangle = \sum_{\mathbf{k}\nu} f^{\sigma}_{\mathbf{k}\nu} c^{\sigma}_{\mathbf{k}\nu,\beta n} c^{\sigma *}_{\mathbf{k}\nu,\beta' n'}, \tag{15}$$

where $c^{\sigma}_{\mathbf{k}\nu,\beta' n'} = \langle\beta'\widetilde{n'}\sigma\rangle\Psi^{\sigma}_{\mathbf{k}\nu}\rangle$ is the LCPAO coefficient. If the overlap integrals between the basis orbitals are negligible, that is, $S_{\alpha m,\beta n} \approx \delta_{\alpha\beta}\delta_{mn}$, then the occupation number matrix for the full local projector becomes equal to the density matrix or the "on-site" occupation matrix for each subshell α. Since, however, the overlap integrals cannot be neglected for the nonorthogonal basis, the choice of the local projectors will affect the occupation number matrix. The *on-site*[31] and *full*[32] occupation number matrices have been used in the previous implementations of LDA+*U* methods based on the nonorthogonal LCAO basis.[34] While the *full* version of the occupation number matrix takes care of the full wavefunction overlaps between the atoms containing localized $3d$-or $4f$-orbitals and their neighbors, the *on-site* version totally neglect them. The *on-site* version of the occupation number matrix has been implemented by Eschrig and coworkers into the full-potential local-orbital code and applied to planar cuprate systems,[31] and the *full* version was used by Pickett and co-workers for the estimation of *U*-value from local-orbital based density functional calculations.[32] However, as Pickett and co-workers have pointed out, the occupation number matrix defined by either the *full* or *on-site* projectors does not satisfy the sum rule, i.e., the trace of the occupation number matrices do not take account of the total number of electrons.[32]

Now let us introduce a new definition of the local projector and the corresponding occupation number matrix, so-called a "*dual*" representation:

$$\hat{P}^{\sigma}_{\alpha mm'}(\text{dual}) = \frac{1}{2}(|\widetilde{\alpha m'\sigma}\rangle\langle\alpha m\sigma| + |\alpha m'\sigma\rangle\langle\widetilde{\alpha m\sigma}|), \tag{16}$$

$$\mathsf{n}^{\sigma}_{\alpha mm'} = \frac{1}{2}\sum_{\beta n}(\rho^{\sigma}_{\alpha m,\beta n} S_{\beta n,\alpha m'} + S_{\alpha m,\beta n}\rho^{\sigma}_{\beta n,\alpha m'}). \tag{17}$$

The *dual* version of the occupation number matrix takes the intermediate form of the *full* and *on-site* versions. The symmetrization in the projector defined by Eq. (16) is employed in order to make sure that the resultant effective nonlocal potential becomes Hermitian. More importantly it is noted that the *dual* occupation number satisfies the sum rule exactly:

$$\sum_{\alpha\sigma}\mathrm{Tr}(\mathsf{n}^{\sigma}_{\alpha}) = \frac{1}{2}\sum_{\alpha\sigma}\{\mathrm{Tr}(\rho^{\sigma}\mathsf{S}) + \mathrm{Tr}(\mathsf{S}\rho^{\sigma})\}$$
$$= N_{\mathrm{ele}}, \tag{18}$$

where $\mathsf{n}^{\sigma}_{\alpha}$, ρ^{σ}, and S represent the matrix form of $\mathsf{n}^{\sigma}_{\alpha mm'}$, $\rho^{\sigma}_{\alpha m,\beta n'}$, and $S_{\beta n,\alpha m'}$, respectively. Indeed, in the dual formulation, the occupation number matrix is treated consistently in the same way as in the Mulliken population analysis.[35] Though, within the LCAO formalism, there has been no satisfactory way of defining the atomic density from the point of the sum rule. Contrary to the *on-site* and *full* cases, the *dual* representation can provide a proper way of counting the occupation number for the nonorthogonal basis. The same

concern remains for the case of the LMTO formulation of LDA+U. In the atomic sphere approximation (ASA), which is often used in LMTO, called as LMTO-ASA, a rather artificial cutoff is required for the description of wave-function tails outside the muffin-tin sphere,[36] but the treatments of the overlaps between neighbors is not clearly specified.

C. Effective potential and force

The effective potentials and forces on atoms have contributions from the LDA+U correction energy in Eq. (5). The derivative of the correction energy of Eq. (5) with respect to the LCAO coefficient $c^{\sigma,*}_{\nu,tn}$ is given by

$$\frac{\partial E_U}{\partial c^{\sigma,*}_{\nu,\beta n}} = \sum_{\alpha m m'} v^{\sigma}_{U,\alpha m m'} \frac{\partial \mathsf{n}^{\sigma}_{\alpha m m'}}{\partial c^{\sigma,*}_{\nu,\beta n}} \tag{19}$$

with $v^{\sigma}_{U,\alpha m m'} \equiv U_{\alpha}(1/2\,\delta_{mm'} - \mathsf{n}^{\sigma}_{\alpha m m'})$. The derivative of $\mathsf{n}^{\sigma}_{\alpha m m'}$ with respect to $c^{\sigma,*}_{\mathbf{k}\nu,\beta n}$ depends on the *on-site*, *full*, and *dual* formulations. From Eqs. (13), (14), and (17) we obtain a simple expression of the effective nonlocal potentials in terms of the local projectors:

$$\hat{v}^{\sigma}_{U} = \sum_{\alpha m m'} v^{U,\sigma}_{\alpha m m'} \hat{P}^{\sigma}_{\alpha m m'}(R), \tag{20}$$

where R=*on-site*, *full*, or *dual*. Here it is noted that the local projector $\hat{P}^{\sigma}_{\alpha m m'}(R)$ of the effective potential $\hat{v}^{\sigma}_{U}$ is independent of the choice of the double counting term, where $\hat{v}^{\sigma}_{U}$ may change but $\hat{P}^{\sigma}_{\alpha m m'}(R)$ remains unchanged even if we adopt a different mean field form instead of the fully localized limit discussed in Eq. (3).

It is obvious that the *full*- and *on-site* effective potentials are Hermitian. Further it can be easily verified that the *dual*-effective potential is also Hermitian due to the symmetrized form of the projector of Eq. (16):

$$\begin{aligned}
&\langle \beta n\sigma | \hat{v}^{\sigma}_{U} | \beta' n'\sigma \rangle \\
&= \frac{1}{2}\sum_{m'} v^{\sigma}_{U,\beta n m'} S_{\beta m',\beta' n'} + \frac{1}{2}\sum_{m} S_{\beta n,\beta' m} v^{\sigma}_{U,\beta' m n'} \\
&= \langle \beta' n'\sigma | \hat{v}^{\sigma}_{U} | \beta n\sigma \rangle .
\end{aligned} \tag{21}$$

Similarly the contribution of the correction energy of Eq. (5) to the force on the kth atom can be evaluated by

$$\begin{aligned}
\frac{\partial E_U}{\partial \mathbf{R}_k} &= \sum_{\sigma,\alpha m m'} \frac{\partial E_U}{\partial \mathsf{n}^{\sigma}_{\alpha m m'}} \frac{\partial \mathsf{n}^{\sigma}_{\alpha m m'}}{\partial \mathbf{R}_k} \\
&= \sum_{\sigma,\alpha m m'} v^{\sigma}_{U,\alpha m m'} \frac{\partial \mathsf{n}^{\sigma}_{\alpha m m'}}{\partial \mathbf{R}_k} \\
&= \sum_{\mathbf{k}\sigma\nu} f_{\mathbf{k}\nu} \sum_{\beta n,\beta' n'} \left\{ \frac{\partial c^{\sigma,*}_{\mathbf{k}\nu,\beta n}}{\partial \mathbf{R}_k} \langle \beta n\sigma | \hat{v}^{\sigma}_{U} | \beta' n'\sigma \rangle c^{\sigma}_{\mathbf{k}\nu,\beta' n'} \right. \\
&\quad + c^{\sigma,*}_{\mathbf{k}\nu,\beta n} \langle \beta n\sigma | \hat{v}^{\sigma}_{U} | \beta' n'\sigma \rangle \frac{\partial c^{\sigma}_{\mathbf{k}\nu,\beta' n'}}{\partial \mathbf{R}_k} \\
&\quad \left. + c^{\sigma,*}_{\mathbf{k}\nu,\beta n} c^{\sigma}_{\mathbf{k}\nu,\beta' n'} \frac{\partial \langle \beta n\sigma | \hat{v}^{\sigma}_{U} | \beta' n'\sigma \rangle}{\partial \mathbf{R}_k} \right\}.
\end{aligned} \tag{22}$$

Considering $\hat{H}_{\mathbf{k}} c_{\mathbf{k}\nu} = \epsilon_{\nu} \hat{S}_{\mathbf{k}} c_{\mathbf{k}\nu}$ and $\hat{C}^{\dagger}_{\mathbf{k}} \hat{S}_{\mathbf{k}} \hat{C}_{\mathbf{k}} = \hat{\mathrm{I}}$, the first and second terms in Eq. (22) can be transformed into the derivative of the overlap matrix. In the third term of Eq. (22) the differentiation of the overlap matrix is required, since the expression of $\mathsf{n}^{\sigma}_{\alpha}$ excludes v_U. Also, it is noted that in the *on-site* represention no modification is required in the evaluation of force compared to the LDA case due to the disappearance of the third term.

D. Computational details

We carried out electronic structure calculations for the periodic unit cell of transition metal mono-oxide systems based on the density-functional theory (DFT) within local spin-density approximation (LSDA)[37] and LDA+U by employing a linear-combination-of-localized-pseudo-atomic orbitals (LCPAO) method.[26] We used $6\times6\times6$ k-points and the Ceperley-Alder exchange-correlation energy functional as parameterized by Perdew and Zunger.[37] Double valence orbitals were used as a basis set of oxygen, which are generated by a confinement potential scheme[26] with the cutoff radius of 4.5 a.u. For transition metal (TM) atoms we used double valence and polarization orbitals with the cutoff radius of 5.5 a.u. The effect of the different selections of the basis set for transition metal atoms especially within the LDA+U scheme is investigated and discussed in the next section. Troullier-Martins type pseudopotentials[38] with a partial core correction[39] were used to replace the deep core potentials by norm-conserving soft potentials in a factorized separable form with multiple projectors proposed by Blochl.[40] In this pseudopotential generation, the semicore $3p$ electrons for TM atoms were included as valence electrons in order to take into account the contribution of the semicore states to the electronic structures. The real space grid techniques[21] were used with the energy cutoff of 160 Ry in numerical integrations and the solution of the Poisson equation using fast Fourier transformations (FFT). In addition, the projector expansion method was employed to accurately calculate three-center integrals associated with the deep neutral atom potential with $L_{\max}=6$ and $N_{\mathrm{rad}}=4$.[27] All the DFT calculations were performed using our DFT code, OpenMX, which is designed for the realization of large-scale DFT calculations.[41]

III. TRANSITION METAL MONO-OXIDES

A. Band gaps, magnetic moments, and band structures

Table I lists the band gaps for a series of typical transition-metal mono-oxide bulk systems, i.e., MnO, FeO, CoO, and NiO, as calculated by employing LSDA and LDA+U based on the *dual* formalism. Similarly to the previous LDA LDA+U calculation results, the typical increase of the band gaps is observed for the finite $\bar{U}$ values. The magnitudes of the gaps and the effective $\bar{U}$ are well compared in a reasonable agreement with experimental results as

TABLE I. Calculated band gaps of MnO, FeO, CoO, and NiO as a function of $\bar{U}$ values. Here we use the dual representation for the description of the on-site density matrix.

$\bar{U}$ (eV)	MnO	FeO	CoO	NiO
0	0.04	0.00	0.00	0.36
2	1.68	0.76	1.20	1.56
4	2.12	1.96	2.20	2.53
6	4.21	2.77	3.01	3.89
Calc. (LSDA)	0.8[a]	0.0[a]	0.0[a]	0.2[a]
Calc. (LDA+*U*)	3.5[b]	3.2[c]	3.2[d]	3.1[e]
Expt.	3.6-3.8[f]	2.4[g]	2.4[h]	4.0[i], 4.3[j]

[a]Reference 52.
[b]Reference 6; $\bar{U}$=6.04 is used.
[c]Reference 6; $\bar{U}$=5.91 is used.
[d]Reference 6; $\bar{U}$=6.88 is used.
[e]Reference 6; $\bar{U}$=7.05 is used.
[f]Reference 53.
[g]Reference 54.
[h]Reference 55.
[i]Reference 56.
[j]Reference 57.

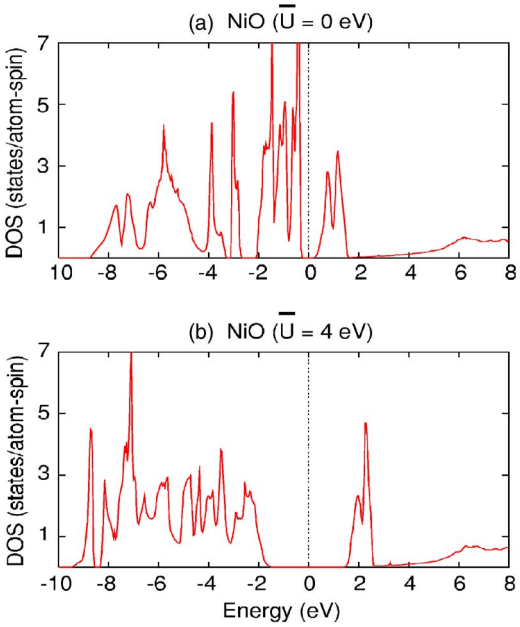

FIG. 1. (Color online) The effect of on-site Coulomb interaction in total density of states (DOS) of bulk NiO. (a) and (b) correspond to $\bar{U}$=0 and 4 eV, respectively. Fermi level is set to be zero (vertical dotted line).

well as the previous calculations. (See the references listed in Table I.) Since the effect of the $\bar{U}$ values depends on the calculational methods in detail, however, the direct comparison of the results at a fixed value of $\bar{U}$ may not be appropriate.

Table II illustrates the enhancement of the magnetic moments. As expected, the larger the $\bar{U}$ values, the larger magnetic moments are obtained and the values are in good agreement with experiments and previous calculations as listed in Table II. The difference between the moments from Mulliken and Voronoi charge analysis will be discussed in the next section. Figure 1 demonstrates the change of the total density of states of bulk NiO as the on-site effective Coulomb interaction $\bar{U}$ increases from 0 to 4 eV. By taking account of the on-site correlation effect, Ni-*d* bands below (above) the Fermi level are shifted to the lower (higher) energy level, resulting in a notable gap, and the e_g bands of majority spin move down below to the t_{2g}. The calculated band structure is given in Fig. 2, which is well compared with previous calculations and experiments.[29] The exchange interaction parameters between the nearest neighbor Ni sites, J_1, and the next nearest neighbors, J_2, have been estimated by using the total energy method[42] ($\bar{U}$=5 eV used). The obtained result, J_1=1.8 meV and J_2=−16 meV, is in reasonable agreement with the previous calculations by LSDA-SIC (J_1=2.3 and J_2=−12 meV), LSDA-SIC with empty spheres (J_1=1.8 and J_2=−11 meV), LSDA (J_1=5.3 and J_2=−106 meV), and the experiment (J_1=1.4 and J_2=−19 meV)[42] as well.

TABLE II. Magnetic moment at the Ni site in μ_B unit as a function of $\bar{U}$ values and the definition of occupation number.

	Mulliken			Voronoi			
$\bar{U}$ (eV)	Full	Dual	On-site	Full	Dual	On-site	Other group results
0	1.30	1.30	1.30	1.28	1.28	1.28	1.0 ($\bar{U}$=0.0)[a]
2	1.48	1.54	1.59	1.46	1.51	1.55	
4	1.59	1.66	1.71	1.55	1.61	1.66	
6	1.66	1.74	1.79	1.62	1.69	1.72	1.59 ($\bar{U}$=6.9)[b]
Expt.							1.77[c], 1.64[d], 1.90[e]

[a]Reference 52.
[b]Reference 6.
[c]Reference 58.
[d]Reference 59.
[e]Reference 60.

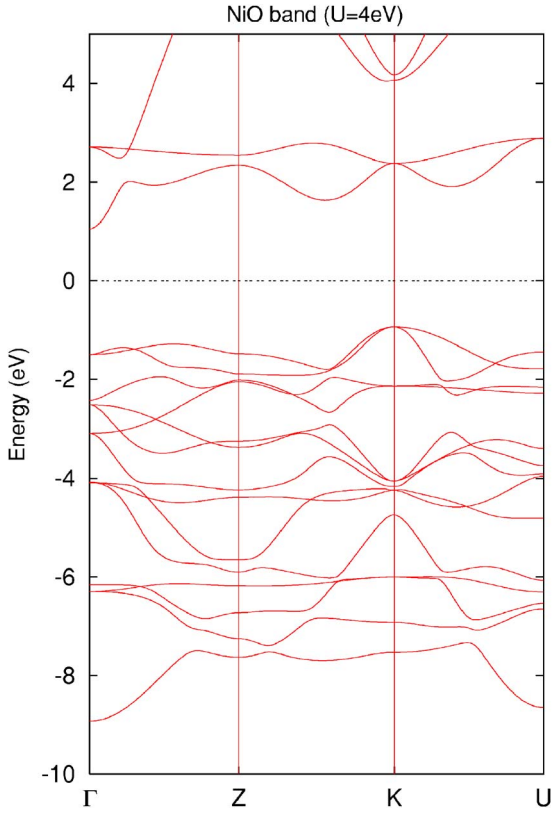

FIG. 2. (Color online) Band dispersion of NiO. $\bar{U}$=4 eV is used. Fermi level is set to be zero (horizontal dotted line).

B. Occupation number matrix

In Sec. II B, we discussed the definitions of occupation number matrices in the formulation of LDA+U methods especially within the nonorthogonal LCAO formalism. Figure 3 shows the projected density-of-states (PDOS) of bulk NiO as obtained from the calculations with the use of the (a) *on-site*, (b) *dual*, and (c) *full* representations of the local projection operators in Eqs. (9), (16), and (10), respectively.

Apparent differences among the PDOS results of the Ni 3d e_g-, t_{2g}-, and O 2p-states for the use of three different local projectors are the reduction of the band gap as the local projector changes from (a) *on-site* to (b) *dual* to (c) *full* representations. The similar trend is also seen in the magnetic moments of Table II; the *on-site* representation gives the larger magnetic moments than *dual* and *full*. When the *full* representation is used, the imposed value of $\bar{U}$ on TM-d orbitals is shared with surrounding orbitals, such as O-p, via the overlap matrix, and consequently we have an effectively smaller $\bar{U}$ value than the case of using the same $\bar{U}$ but with the *on-site* density. The results of the *dual* representation stay always in-between *full* and *on-site* for both the magnetic moment (Table II) and the PDOS results (Fig. 3). It is partly because the *dual* projector is defined as the intermediate form of *full* and *on-site* [see Eqs. (9), (10), and (16)]. Overall features of the PDOS of bulk NiO presented in Fig. 3 are consistent with the previous results obtained by the LDA +U[6,28,29] and self-consistent GW (SCGW) methods.[43]

Apart from the change of band gaps, one can observe that there are subtle changes of the PDOS weights near the Fermi

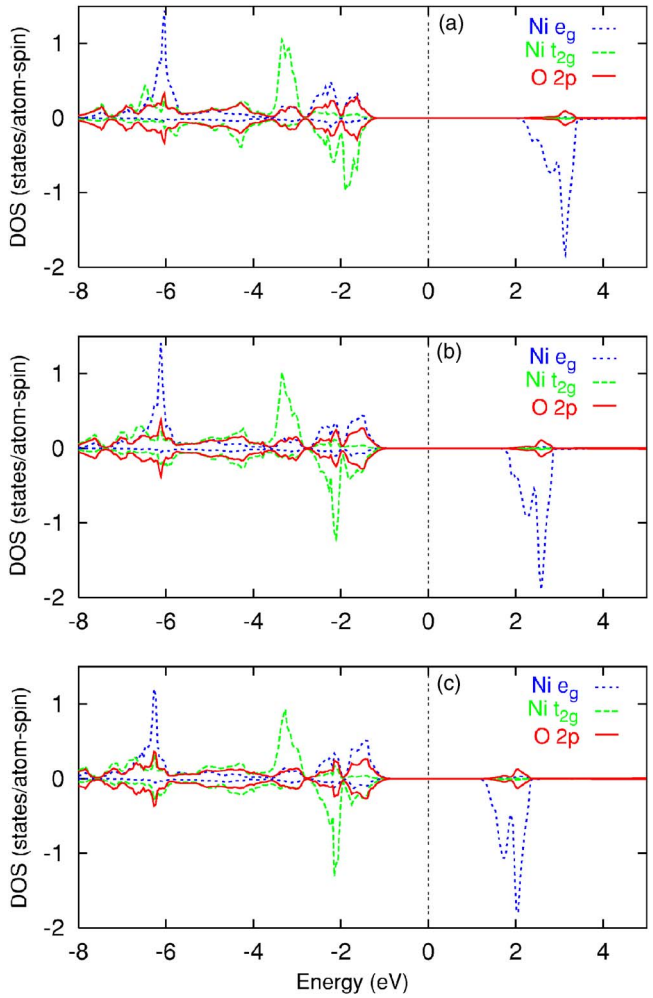

FIG. 3. (Color online) The dependence of projected DOS of bulk NiO on the representation of local projector: (a) *on-site*, (b) *dual*, and (c) *full*. Dotted (blue) and dashed (green) lines represent Ni e_g and t_{2g} states, respectively, and solid (red) lines correspond to O 2p. Upper and lower panels correspond to the up- and down-spin, respectively. $\bar{U}$=4 eV is used. Fermi level is set to be zero (vertical dotted line).

level. While there is almost no change in the relative weight distribution of O 2p PDOS, the PDOS weight of Ni e_g-states just below the gap becomes enhanced significantly and the t_{2g}-state becomes shifted toward the lower energy, as the orbital overlap is more effective for the $dp\sigma$ hybridizations than the $dp\pi$ ones in the *dual* and *full* representations. Thus it is concluded that the choice of the local projection operators, *on-site*, *dual*, or *full*, affects the electronic structure due to their different treatments of the TM-3d and O-2p hybridizations. Although the general features of LDA+U are kept in all three representations, the use of *dual* representation is possibly important in some critical situation owing to the oversimplification in *on-site* description.

In the use of nonorthogonal LCAO based methods there still remains an issue regarding the local charge analysis due to some ambiguity in the determination of on-site atomic charges. Because of the intersite overlap of orbitals, the contribution of the nonzero overlap terms to the on-site density

needs to be decomposed into either the site i or the site j. The Mulliken charge analysis may be one of the most popular methods[35] in which a half of the overlap term is assigned to the i-site and the other half to the j-site. However, the Mulliken analysis is still somehow artificial in the treatments of wave function and charge as well. Although there has been no legitimate way to resolve the ambiguity, one can try a popular method based on the real space partitioning such as the Voronoi method.[44]

In fact a real space partition method such as Voronoi analysis can provide information supplementary to the Mulliken analysis. The estimation of the on-site magnetic moment depends on the way of on-site charge analysis. In Table II, we compare the results of both Mulliken and Voronoi charge analysis. Though the Mulliken analysis tends to give large magnetic moments compared to that of Voronoi, both results are rather reasonable when compared to previous studies. However, it is observed that, when the multiple orbitals are used for calculation, the Mulliken method tends to overestimate the magnetic moment, which is attributed to the longer tails of the multiple orbital basis for both TM and O. Therefore one has to be cautious in the on-site charge or magnetic moment analysis when multiple orbitals are employed for the description of d-orbitals. It is noted that the charge analysis in LMTO-ASA is similar to the Voronoi method rather than the Mulliken one in the sense that the Muffin-tin sphere is used.

C. Choice of the local pseudoatomic orbital (PAO) basis

Often the multiple-zeta and polarization orbitals are adopted in the LCAO-based calculations,[21,45] but it is not clear how the LDA+U calculation will be affected by the use of the multiple-zeta and polarization orbitals. The DOS of NiO calculated by using three different orbital configurations are shown in Fig. 4 where the label $dm(\bar{U}_1,\ldots,\bar{U}_m)fn(\bar{U}_1,\ldots,\bar{U}_n)$ means that the mth d-orbital has the $\bar{U}$ value of $\bar{U}_m$ and nth f-orbital $\bar{U}_n$. For example, $d2(4,2)f1(2)$ denotes that for the first d-orbitals $\bar{U}=4$ eV is used and the second d- and f-orbital, $\bar{U}=2$ eV is used. The result demonstrates that the calculated electronic structure remains robust, not being affected much by the use of additional multiple-zeta and polarization orbitals except a slight modification of the valence band structure. It should be mentioned that the $\bar{U}$ value imposed on the multiple zeta and the polarization orbital is not predetermined.

D. Numerical robustness

As for the numerical aspect, the robustness such as convergence in the self-consistency iterations depends on the definition of the occupation number matrix discussed in Sec. II. From the calculations with three different definitions of the local projectors and the $\bar{U}$ values, the convergence rate of the *on-site* case turns out to be slower than the others. Its slow convergence is attributed to the neglect of the overlap matrix in its definition. In the LCPAO formulation, the KS eigenfunctions corresponding to the on-site d-orbitals are modulated by the orbitals of neighboring sites through the orbital overlaps. Thus, in principle, the orbitals of neighboring sites should be affected by the effective $\bar{U}$ potential imposed on the d-states. Although there is a substantial contribution of the orbitals of neighboring sites to the on-site d-states, however, the effective $\bar{U}$ is imposed only on the d-orbitals due to the neglect of the overlap in the *on-site* representation. The difficulty arising from the neglect of the overlap becomes more serious as the the effective $\bar{U}$ value increases. It is observed that when the very large $\bar{U}$ value is used, the electronic structure of the NiO bulk switches over to an unphysical state exhibiting a quite large charge transfer between Ni and O orbitals. On the other hand, in the other definitions, *full* and *dual*, such an unstable behavior has not been observed even for the large $\bar{U}$ values.

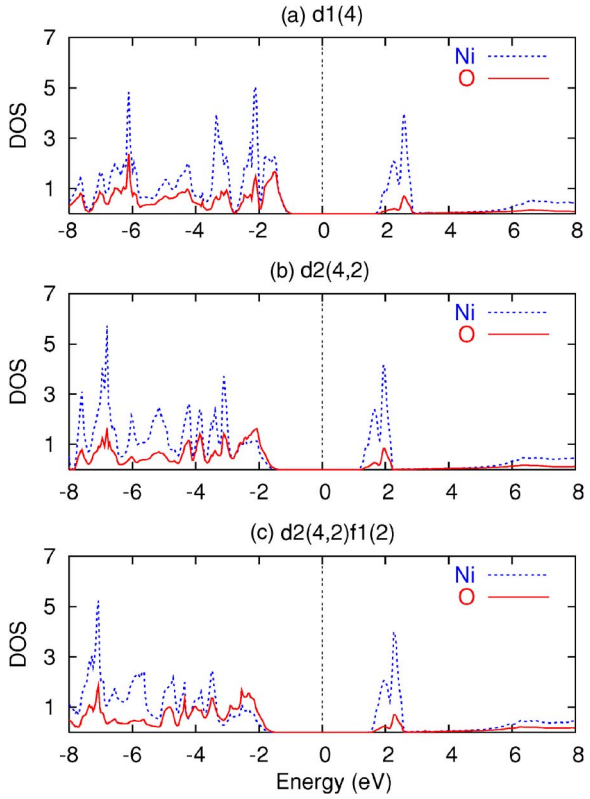

FIG. 4. (Color online) Projected DOS of NiO where the different basis orbitals are used: (a) single zeta orbital for Ni-3d, (b) double zeta and (c) double zeta plus polarization. Dotted (blue) and solid (red) lines represent Ni and O states, respectively. Fermi level is set to be zero (vertical dotted line).

E. Enhancement of orbital polarization

The LDA+U functional can possess multiple local minima due to the degrees of freedom in the configuration space of degenerate orbitals. Since the self-consistent (SC) electronic structure obtained by the LDA+U method can depend on the initial occupancy ratio in the SC calculation, we propose a way of obtaining an orbitally polarized state with a lower energy than that of the nonorbital-polarization state. If degenerate orbital states are occupied with nearly the same occupancy ratio at the first stage of SC steps, it often con-

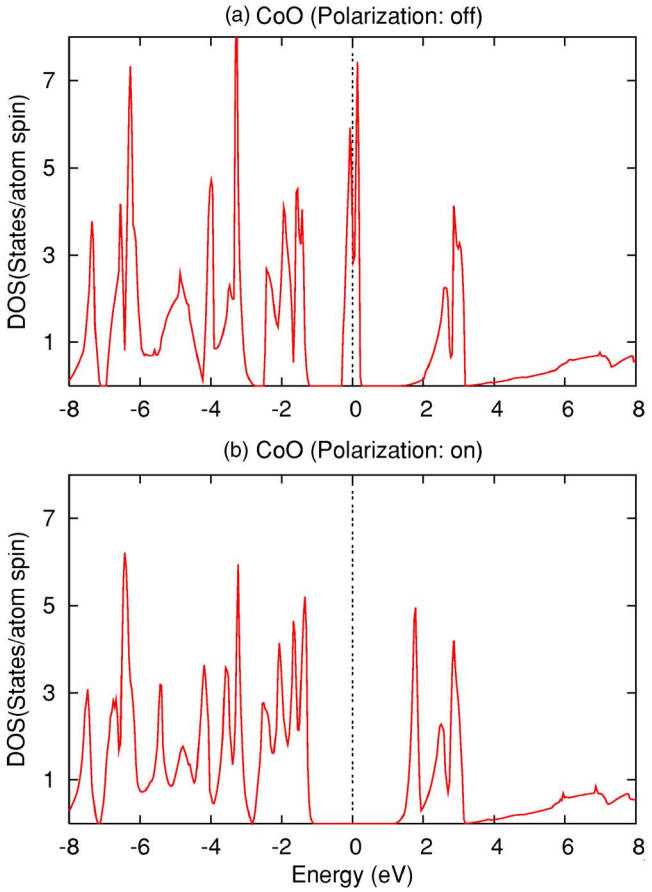

FIG. 5. (Color online) Total DOS of CoO calculated with and without orbital polarization. $\bar{U}$=4 eV is used. Fermi level is set to be zero (vertical dotted line).

verges into a local minimum without any orbital polarization after the SC iteration. On the other hand, it is often more likely that an uneven occupation of degenerate orbitals, i.e., orbital polarization, occurs due to the orbital dependent functional. As an example of such multiple minima situation in the energy functional, we can consider the cobalt monoxide (CoO) bulk, in which the d-states of the cobalt atom are split to t_{2g}- and e_g-states; the five of seven d-electrons occupy the t_{2g}- and e_g-states of the majority spin, and the remaining two d-electrons occupy the t_{2g}-states of the minority spin. In this case, the ground state configuration may depend on the initial occupancy ratios for the t_{2g}-states of the minority spin. When the initial occupancy ratios are chosen to be uniform, the SC iteration leads to the nonorbital polarized state unless any explicit nonuniform distribution of the initial occupancy is introduced, as shown in Fig. 5(a) of the nonorbital polarized of the bulk CoO. Even though the orbital polarization solution can be achieved in the presence of the symmetry break term in the Hamiltonian such as spin-orbit couplings and Jahn-Teller distortions,[46] however, the practical solution with orbital polarization in practice requires some sort of acceleration scheme to overcome the energy barrier in configurational space and to access the *lower* energy minimum of the LDA+U function.

In order to explore such a degree of freedom for the orbital occupation, we developed a general algorithm which guarantees the orbital polarization[47] when it is required. To do this, we propose an occupation redistribution scheme as follows:

$$\text{diagonalize } n^{\sigma}_{\alpha m} = [\mathsf{A}^{\dagger}_{\alpha}\mathsf{n}^{\sigma}_{\alpha}\mathsf{A}_{\alpha}]_{mm}$$

$$n^{\sigma}_{\alpha m}\text{: ascending order} \tag{23}$$

$$\text{summation } D = \sum_{m=-l}^{l} n^{\sigma}_{\alpha m}$$

$$\text{redistribution } n'_{l} = 1,$$

$$n'_{l-1} = 1,$$

$$\ldots, \tag{24}$$

$$n'_{m} = D - (l - m),$$

$$n'_{m-1} = 0,$$

$$\ldots \tag{25}$$

$$\text{where } D = \sum_{m} n'_{m} \tag{26}$$

$$\text{back transform } \mathsf{n}'^{\sigma}_{\alpha} = \mathsf{A}_{\alpha}[n'^{\sigma}_{m}\delta_{mm'}]\mathsf{A}^{\dagger}_{\alpha}. \tag{27}$$

After diagonalizing each subshell matrix consisting of occupation numbers, we introduce a polarized occupation redistribution given by Eq. (25) to induce an orbital polarization explicitly, while keeping Eq. (26). Then, through a back transformation of Eq. (27), an occupation matrix for each subshell with an orbital polarization can be obtained. The proposed scheme can be applicable to general cases: any crystal field, any number of electrons in the subshell, and any orbitals (p,d,f). Once the occupation redistribution step is applied during the first few SC steps only, then no more redistribution steps are required during the subsequent SC steps. Therefore, after the SC iterations, the final results of occupation number distribution should settle on its minimum energy configuration. Even in the case of strong orbital polarization, in principle, the SC method should give a correct ground state, but in practice there may exist a possibility of being trapped in a local minimum. The orbital polarization scheme which we suggested here is a method for assuring the ground state even in a situation where several orbital configurations are almost degenerate. By the comparison of total energies the local trap issue can be resolved.

The total DOS of CoO bulk obtained by this proposed scheme is shown in Fig. 5(b). From the comparison of Figs. 5(a) and 5(b), it is shown that this proposed scheme induces the band gap due to the orbital polarization. In addition, the total energy of the orbital polarization state given by Fig. 5(b) is 1.5 eV/unit-cell lower than that of the nonorbital polarization state of Fig. 5(a), which demonstrates that the occupation redistribution scheme works effectively in search of the lower energy ground state.

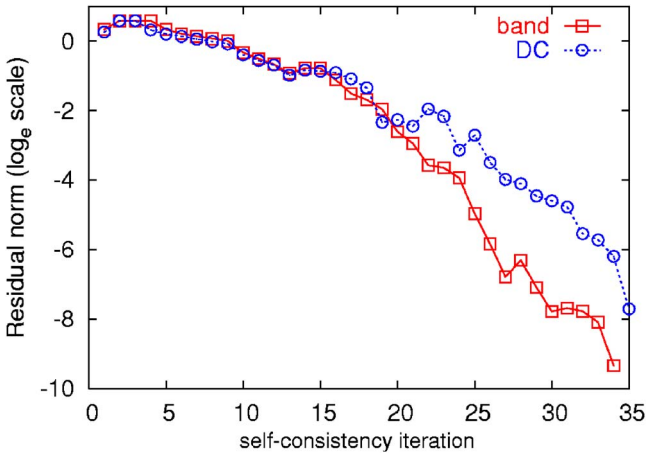

FIG. 6. (Color online) The residual norm of charge density in $\log_e$ scale as a function of SC steps calculated by conventional band method and DC method.

F. Linear-scaling LDA+*U*

The LCPAO method with the LDA+*U* aims at the electronic structure calculations of large-scale correlated systems. When this scheme is combined with a linear-scaling method, the so-called O(*N*) method, the applicability of the scheme can be significantly extended up to large systems more than thousands of atoms. As an illustration of the linear-scaling LDA+*U* calculation, we present a comparison between the conventional *k*-space method and a divide-conquer (DC) O(*N*) method[13,18] with respect to the SC convergence of MnO bulk and the error in the total energy. Figure 6 shows a residual norm of the charge density in the reciprocal space as a function of SC steps. We see that the convergence rate of the DC method is comparable to that of the conventional *k*-space method. The difference in the total energy by the DC calculations compared to that by the *k*-space method was less than 0.0029 (Hartree/atom). Although a primitive cell including four atoms was used in the calculations, the DC method becomes more efficient when the number of atoms in the unit cell exceeds the crossing point N_{cross} at which the computational time by the *k*-space and DC methods intersect with each other. The crossing point N_{cross} can be estimated by $N_c^{3/2}$, where N_c is the number of atoms in the cluster used in the DC method,[18] and it is estimated as $69^{3/2}=573$ in this case. Therefore the illustration clearly suggests that, along with this line, our scheme could provide an efficient method of achieving linear-scaling LDA+*U* calculations of large-scale strong correlated systems.

IV. APPLICATION TO $(NiO)_m/(CoO)_n$ MULTILAYER

Due to the recent progress in the materials deposition technique, intriguing magnetic property appearing at the interface has been vitally studied. One of those systems is the Mott insulator interface such as $(LaTiO_3)/(SrTiO_3)$ (Ref. 48) and $(NiO)_m/(CoO)_n$ interface.[49] For example, Borchers *et al.*[49] performed the neutron diffraction and heat capacity measurements of NiO/CoO superlattice along the [111] direction to understand the exchange coupling and the magnetic proximity effect at the interface. The transition temperature of the superlattice is observed to be in between that of bulk NiO and CoO, and the antiferromagetic order in CoO survives through several layers from the interface even above the Neel temperature of CoO.[49]

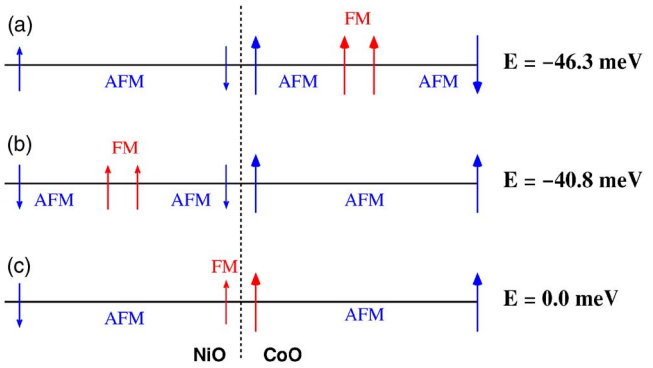

FIG. 7. (Color online) Schematic drawing of magnetic structure of a NiO-CoO multilayer calculated in this study and their total energy: eight layers for NiO and seven for CoO. In AFM ordered structures (blue), FM ordering (red) is placed in the Co (a), Ni (b) layers and at the interface (c), respectively.

As a step toward a large scale application of LDA+*U* methods, we carried out electronic structure calculations for the $(NiO)_m/(CoO)_n$ superlattice structures of [111] interface and the periodic unit cell by using our LDA+*U* method with the *dual* representation of the local projector and $\bar{U}=5$ eV. First, $(NiO)_m/(CoO)_n$ superlattice structures with various values of $m=n$ have been studied up to $m=n=40$, in which the total number of atoms per unit-cell is 160, the comparable size to the experimental ones.[49] Since the AFM ordering is not broken in this case, each layer of CoO and NiO remains independent and a little disturbance of the electronic and magnetic structure does appear at the interface. Ni and Co magnetic moments as well as the local band gap are almost equivalent to the bulk values.

An odd number of mono-oxide layers are, however, expected to frustrate the magnetic orderings and give rise to confined FM bilayers inside the AFM ordered superlattices. To understand the competition of magnetic interactions under frustrated spin configurations, we performed the calculations[50] for three different FM bilayer configurations: (i) FM bilayer inside the CoO layers [Fig. 7(a)], (ii) FM bilayer inside the NiO layers [Fig. 7(b)], and (iii) FM bilayer at the NiO-CoO interface [Fig. 7(c)], and examined the stability of those magnetic structures. It is found that the FM bilayer tends to favor energetically the localization of the FM ordered bilayers within the $(CoO)_n$ layers, which still remains insulating. The result is consistent with the fact that the AFM coupling of CoO is weaker than that of NiO.[49] As shown in Fig. 7, the configuration (a) has a lower total energy than that of (b) and (c) by 5.5 and 46.3 meV, respectively. The relative coulping strength of AFM can be estimated from the total energies of bulk AFM and FM phases. The total energy difference of $E_{tot}(\mathrm{FM})-E_{tot}(\mathrm{AFM})$ for CoO and NiO gives about 196 and 348 meV, respectively, and the values are in reasonable agreement with the previous

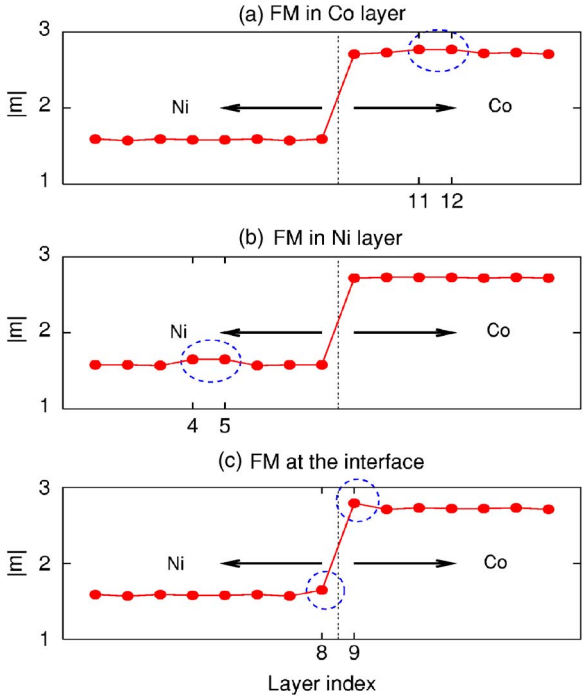

FIG. 8. (Color online) Absolute values of magnetic moment (in μ_B) at the transition metal site as a function of the layer index. FM ordered layers are labeled by the layer index.

calculations.[42,51] Therefore it can be concluded that FM layer is possibly formed in the CoO layer during the experiment materials deposition. Absolute values of the magnetic moment at each transition metal layer are shown in Fig. 8, in which (a)–(c) correspond to those of Fig. 7, respectively. It is noted that there is about 3–5% enhancement of magnetic moment at the FM ordered layers.

V. SUMMARY

We present a nonorthogonal tight-binding formulation of the LDA+U method and its implementation based on the state-of-the-art linear combination of pseudoatomic orbital (LCPAO) method, which is suitable for large-scale O(N) electronic structure calculations based on the density functional theory. To be consistent with the use of a nonorthogonal LCPAO basis in regard to the sum rule of the total number of electrons, we introduce a *dual* representation of the occupation number matrix instead of the *on-site* or *full* representations. For typical transition metal oxide bulk systems, the band gap, magnetic moment, and detailed electronic structures are investigated with respect to the choice of basis orbitals and effective U values as well as the definition of the occupation number matrix. The results are in good agreement with previous theoretical and experimental studies, indicating that the proposed LDA+U scheme coupled with O(N) methods is a quite promising approach for the study of large-scale strongly correlated systems consisting of localized d-electrons. Linear-scaling eigenvalue solver combined with the LDA+U method has been tested and it gives the reasonable result for O(N) LDA+U calculation of the correlated systems including thousands of atoms. Our method is applied to the $(NiO)_m/(CoO)_n$ superlattice to investigate the possibility of stacking fault in the experimental situation and will be applicable to the nanoscale simulation for the correlated electron materials such as surface, interface, cluster, and defect systems.

ACKNOWLEDGMENTS

This work was supported by the KOSEF through CSCMR SRC and by the KRF Grant (MOEHRD KRF-2005-070-C00041). One of us (T.O.) was partly supported by NEDO under the Nanotechnology Materials Program, CREST under the Japan Science and Technology Agency, and NAREGI Nanoscience Project, Ministry of Education, Culture, Sports, Science and Technology, Japan.

*Corresponding author. Email address: jyu@snu.ac.kr

[1] P. Hohenberg and W. Kohn, Phys. Rev. **136**, B864 (1964).
[2] W. Kohn and L. J. Sham, Phys. Rev. **140**, A1133 (1965).
[3] R. G. Parr and W. Yang, *Density Functional Theory of Atoms and Molecules* (Oxford University Press, New York, 1989).
[4] R. M. Martin, *Electronic Stucture: Basic Theory and Practical Methods* (Cambridge University Press, Cambridge, England, 2004).
[5] *Strong Coulomb Correlations in Electronic Structure Calculations: Beyond the Local Density Approximation*, edited by V. I. Anisimov (Gordon and Breach, New York, 2000).
[6] V. I. Anisimov, J. Zaanen, and O. K. Andersen, Phys. Rev. B **44**, 943 (1991).
[7] M. T. Czyzyk and G. A. Sawatzky, Phys. Rev. B **49**, 14211 (1994).
[8] A. G. Petukhov, I. I. Mazin, L. Chioncel, and A. I. Lichtenstein, Phys. Rev. B **67**, 153106 (2003).
[9] J. P. Perdew, R. G. Parr, M. Levy, and J. L. Balduz, Phys. Rev. Lett. **49**, 1691 (1982).
[10] J. Hubbard, Proc. R. Soc. London, Ser. A **281**, 401 (1964).
[11] A. Georges, G. Kotliar, W. Krauth, and M. J. Ronzenberg, Rev. Mod. Phys. **68**, 13 (1996), and references therein.
[12] V. I. Anisimov, F. Aryasetiawan, and A. I. Lichtenstein, J. Phys.: Condens. Matter **9**, 767 (1997), and references therein.
[13] W. Yang, Phys. Rev. Lett. **66**, 1438 (1991).
[14] S. Goedecker and L. Colombo, Phys. Rev. Lett. **73**, 122 (1994).
[15] G. Galli and M. Parrinello, Phys. Rev. Lett. **69**, 3547 (1992).
[16] X.-P. Li, R. W. Nunes, and D. Vanderbilt, Phys. Rev. B **47**, 10891 (1993); M. S. Daw, *ibid.* **47**, 10895 (1993).
[17] T. Ozaki and K. Terakura, Phys. Rev. B **64**, 195126 (2001).
[18] T. Ozaki (unpublished).
[19] S. Goedecker, Rev. Mod. Phys. **71**, 1085 (1999), and references therein.
[20] O. F. Sankey and D. J. Niklewski, Phys. Rev. B **40**, 3979 (1989).

[21] J. Junquera, O. Paz, D. Sanchez-Portal, and E. Artacho, Phys. Rev. B **64**, 235111 (2001); J. M. Soler, E. Artacho, J. D. Gale, A. Garcia, J. Junquera, P. Ordejon, and D. Sanchez-Portal, J. Phys.: Condens. Matter **14**, 2745 (2002), and references therein.
[22] E. Anglada, J. M. Soler, J. Junquera, and E. Artacho, Phys. Rev. B **66**, 205101 (2002).
[23] S. D. Kenny, A. P. Horsfield, and H. Fujitani, Phys. Rev. B **62**, 4899 (2000).
[24] C. K. Gan, P. D. Haynes, and M. C. Payne, Phys. Rev. B **63**, 205109 (2001).
[25] J. D. Talman, Phys. Rev. Lett. **84**, 855 (2000).
[26] T. Ozaki, Phys. Rev. B **67**, 155108 (2003); T. Ozaki and H. Kino, *ibid.* **69**, 195113 (2004); T. Ozaki and H. Kino, J. Chem. Phys. **121**, 10879 (2004).
[27] T. Ozaki and H. Kino, Phys. Rev. B **72**, 045121 (2005).
[28] A. B. Shick, A. I. Liechtenstein, and W. E. Pickett, Phys. Rev. B **60**, 10763 (1999).
[29] O. Bengone, M. Alouani, P. Blochl, and J. Hugel, Phys. Rev. B **62**, 16392 (2000).
[30] See, for example, Z. Fang and K. Terakura, Phys. Rev. B **64**, 020509(R) (2000); F. Zhou, C. A. Marianetti, M. Cococcioni, D. Morgan, and G. Ceder, *ibid.* **69**, 201101(R) (2004); F. Zhou, M. Cococcioni, C. A. Marianetti, D. Morgan, and G. Ceder, *ibid.* **70**, 235121 (2004); M. Cococcioni and S. de Gironcoli, *ibid.* **71**, 035105 (2005).
[31] H. Eschrig, K. Koepernik, and I. Chaplygin, J. Solid State Chem. **176**, 482 (2003).
[32] W. E. Pickett, S. C. Erwin, and E. C. Ethridge, Phys. Rev. B **58**, 1201 (1998).
[33] S. L. Dudarev, G. A. Botton, S. Y. Savrasov, C. J. Humphreys, and A. P. Sutton, Phys. Rev. B **57**, 1505 (1998).
[34] It should be noted that, in previous literatures, the terms of *on-site* and *full* have been used to carry out different meanings from ours. Sometimes another word such as *Mulliken* had been introduced. Here we use these terms as the ones defined in the text.
[35] R. S. Mulliken, J. Chem. Phys. **23**, 1833 (1955).
[36] O. K. Andersen, Z. Pawlowska, and O. Jepsen, Phys. Rev. B **34**, 5253 (1986).
[37] D. M. Ceperley and B. J. Alder, Phys. Rev. Lett. **45**, 566 (1980); J. P. Perdew and A. Zunger, Phys. Rev. B **23**, 5048 (1981).
[38] N. Troullier and J. L. Martins, Phys. Rev. B **43**, 1993 (1991).
[39] S. G. Louie, S. Froyen, and M. L. Cohen, Phys. Rev. B **26**, 1738 (1982).
[40] P. E. Blochl, Phys. Rev. B **41**, 5414 (1990).
[41] Our DFT code, OpenMX, the primitive orbitals, and pseudopotentials ranging from H to Kr used in this study are available on a web site (http://staff.aist.go.jp/t-ozaki/) in the constitution of the GNU General Public Licence.
[42] D. Kodderitzsch, W. Hergert, W. M. Temmerman, Z. Szotek, A. Ernst, and H. Winter, Phys. Rev. B **66**, 064434 (2002).
[43] S. V. Faleev, M. van Schilfgaarde, and T. Kotani, Phys. Rev. Lett. **93**, 126406 (2004).
[44] A. D. Becke and R. M. Dickson, J. Chem. Phys. **89**, 2993 (1988).
[45] See, for example, P. Fulde, *Electron Correlations in Molecules and Solids* (Springer-Verlag, Berlin, 1991).
[46] M. R. Castell, S. L. Dudarev, G. A. D. Briggs, and A. P. Sutton, Phys. Rev. B **59**, 7342 (1999).
[47] It is found that the use of a large value of thermal broadening and/or *k*-space mixing disturb the t_{2g} symmetry existing in the real space and induce the orbital polarization in CoO as a result. Nevertheless a more general scheme to induce the orbital polarization is required.
[48] A. Ohtomo and H. Y. Hwang, Nature (London) **427**, 423 (2004).
[49] J. A. Borchers, M. J. Carey, R. W. Erwin, C. F. Majkrzak, and A. E. Berkowitz, Phys. Rev. Lett. **70**, 1878 (1993); E. N. Abarra, K. Takano, F. Hellman, and A. E. Berkowitz, *ibid.* **77**, 3451 (1996).
[50] We calculated the systems using both eigenvalue solvers (DC and conventional band methods) and obtained the consistent result while the presented are from the band method.
[51] M. D. Towler, N. L. Allan, N. M. Harrison, V. R. Saunders, W. C. Mackrodt, and E. Apra, Phys. Rev. B **50**, 5041 (1994).
[52] K. Terakura, T. Oguchi, A. R. Williams, and J. Kübler, Phys. Rev. B **30**, 4734 (1984).
[53] R. N. Iskenderov *et al.*, Sov. Phys. Solid State **10**, 2031 (1969); L. Messick, W. C. Walker, and R. Glosser, Phys. Rev. B **6**, 3941 (1972).
[54] H. K. Bowen *et al.*, J. Solid State Chem. **12**, 355 (1975).
[55] R. J. Powell and W. E. Spicer, Phys. Rev. B **2**, 2182 (1970).
[56] G. A. Sawatzky and J. W. Allen, Phys. Rev. Lett. **53**, 2339 (1984).
[57] S. Hufner *et al.*, Solid State Commun. **52**, 793 (1984).
[58] B. E. F. Fender *et al.*, J. Chem. Phys. **48**, 990 (1968).
[59] H. A. Alperin, J. Phys. Soc. Jpn. **17**, 12 (1962).
[60] A. K. Cheetham and D. A. O. Hope, Phys. Rev. B **27**, 6964 (1983).